ORIGINAL PAPER

Photoelectrochemical reaction of biomass-related compounds in a biophotochemical cell comprising a nanoporous TiO_2 film photoanode and an O_2-reducing cathode

Hirohito Ueno · Junichi Nemoto · Keita Ohnuki ·
Mizuki Horikawa · Mikio Hoshino · Masao Kaneko

Abstract Photoelectrochemical decomposition of bio-related compounds such as ammonia, formic acid, urea, alcohol, and glycine by a biophotochemical cell (BPCC) comprising a nanoporous TiO_2 film photoanode and an O_2-reducing cathode generating simultaneously electrical power was investigated. The bio-related compounds studied were all photodecomposed by the present BPCC when they were either liquid or soluble in water. It was shown that ethanol exhibits similar characteristics both under 1 atm O_2 and air as studied by cyclic voltammograms. Although the present BPCC utilizes only UV light, a solar simulator at AM 1.5G and 100 mW cm^{-2} light intensity gave also moderate photocurrent–photovoltage (J–V) characteristics with about 2/5 of the short circuit photocurrent (J_{sc}) values (J_{sc}) of that under a Xe lamp irradiation at the intensity of 503 mW cm^{-2}. It was demonstrated that varieties of bio-related compounds can be used as a direct fuel simultaneously for photodecomposition and electrical power generation. The charge transport processes in the BPCC operation were analyzed using glycine by an alternating current impedance spectroscopy, showing that the charge transfer reactions on the photoanode and the cathode surfaces compose the major resistance for the cell performance.

H. Ueno · J. Nemoto · M. Kaneko (✉)
The Institute of Biophotochemonics Co. Ltd, 2-1-1 Bunkyo, Mito, Ibaraki 310-8512, Japan
e-mail: kaneko@biophotochem.co.jp

K. Ohnuki · M. Horikawa
Ibaraki University, 2-1-1 Bunkyo, Mito, Ibaraki 310-8512, Japan

M. Hoshino
REC R&D Inc, 3-10-25-301 Maruyamadai, Wako, Saitama 351-0112, Japan

1 Introduction

Photoelectrochemical reactions at semiconductor electrodes were investigated before the 1960s [1], and the study on a crystalline n-TiO_2 photoanode to photodecompose water by UV light attracted great attention in related research areas [2]. Organic compounds have also been photodecomposed by using crystalline TiO_2 photoanodes [3, 4]. A crystalline n-TiO_2 semiconductor forms a kind of Schottky junction at the TiO_2/aqueous electrolyte interface, the photogenerated holes oxidize organic compounds on the TiO_2 surface, and the photogenerated electrons reduce protons to produce H_2 at a counter electrode. However, without applied potential the photoelectrochemical reactions were not efficient enough, so that these reactions have mostly been investigated under applied potential conditions. In the beginning of the 1990s, a nanoporous TiO_2 thin film was successfully applied to fabricate a dye-sensitized solar cell (DSSC) that gave more than 10% energy conversion efficiency without applied potential [5]. In this DSSC, however, the TiO_2 film works only in an organic liquid electrolytes solution, while working as an electron acceptor for the photoexcited dye compound and at the same time as an electron-conducting material rather than working as a kind of Schottky junction semiconductor. The photoreactivity of a nanoporous TiO_2 film having a large area of effective interface between TiO_2 and water is an

interesting and important issue toward applications, but the details require further investigation.

Biomass and bio-related compounds are attracting a great deal of attention as a renewable energy resource for reducing carbon dioxide (CO_2) emission, but their energy conversion into practical energy also requires further investigation. As one candidate for such energy conversion, we proposed direct photoelectrochemical energy conversion of biomass and bio-related compounds into electrical energy by utilizing a BPCC comprising a nanoporous TiO_2 photoanode and an O_2-reducing cathode [6–8]. For this purpose, it is important not only to photodecompose the compounds at a semiconductor photoanode surface but also to reduce O_2 at a counter cathode electrode to generate electrical power instead of reducing protons into H_2 there. In addition to such energy problem, biomass wastes are serious pollutants all over the world, so finding a means to entirely decompose them into harmless compounds is an urgent issue.

Many biomasses and their model compounds including polymeric compounds such as polysaccharides, proteins, cellulose, lignin, saccharides, etc., can be decomposed photoelectrochemically generating simultaneously electrical power by using the BPCC when they are either liquid or used as an aqueous solution or in suspension [6–8]. However, the details of the cyclic voltammogram (CV) and the photocurrent–photovoltage (J–V) characteristics require further investigation. The present article reports details of the CVs under dark and irradiation as well as the J–V characteristics of the BPCC using biomass-related compounds such as ammonia, formic acid, urea, alcohol, and amino acid. In addition, the charge transport processes in the BPCC were investigated by alternating current impedance spectroscopy taking glycine as a probe compound.

2 Experimental

2.1 Materials

A nanoporous TiO_2 film was prepared as follows: 12 g TiO_2 (P-25, received from Japan Aerosil Co., Ltd.) and acetylacetone (0.4 ml) were mixed well in a mortar while slowly adding 20 ml of water. Triton X-100 (0.2 ml) detergent was added and further mixed well with the TiO_2 slurry, and then the mixture was sonicated for 30 min. This mixture was spin-coated (2,000 rpm) on an FTO (fluorine doped conducting glass, resistance 9 ohm/sq.cm, purchased from Asahi Glass Co. Ltd.) electrode (2 × 1 cm) for about 10 s to obtain a 1 × 1 cm area of a nanoporous TiO_2 film, and the film was dried at 100 °C for 30 min. This procedure was repeated until the film thickness becomes 10 μm,

and finally, the film was calcined at 450 °C for 30 min. As an O_2 reduction cathode, Pt-black was deposited electrochemically from $K_2[PtCl_6]$ on a Pt foil (size 1 cm × 1 cm, coated on both sides). All the chemicals used in the research were commercially available purest grade and used as received.

2.2 Measurements

As an example, ammonia was used as a reactant and photodecomposed by a nanoporous TiO_2 film photoanode. Cyclic voltammogram (CV) was measured as follows: the TiO_2 film electrode (1 cm × 1 cm), a Pt-black coated Pt plate cathode (1 cm × 1 cm), and an Ag|AgCl reference electrode were soaked in a 10 M (M = mol L^{-1}) NH_3 aqueous solution (5 mL, pH 12) in a 10 mL cylindrical Pyrex glass cell (Cell 1) containing also 0.1 M Na_2SO_4 electrolyte. O_2 gas was bubbled into the water for 30 min to substitute the air by O_2 when it is needed. It was confirmed that the Pyrex glass cell transmitted light with a wavelength longer than 300 nm. The TiO_2 film was irradiated with a 500 W Xenon (Xe) lamp through an IR cutoff filter (IRA-25S) (light intensity 503 mW cm^{-2}, UV light intensity about 40 mW cm^{-2}). The gases (N_2, H_2, and O_2) evolved were analyzed by a gas chromatograph (Shimadzu, GC-2014) with a molecular sieve (5 A) column at 40 °C using argon carrier gas. CO_2 was analyzed with a silica gel column at 80 °C using He carrier gas (Shimadzu, GC-8A). All the photoelectrochemical reactions were performed at 25 °C. The photocurrent–photovoltage (J–V) characteristics were measured by a two electrodes system, i.e., with a nanoporous TiO_2 photoanode and a Pt plate cathode.

In order to analyze multistep charge transport processes in a BPCC, alternating current impedance spectroscopy was conducted using a 0.5 M glycine (+0.1 M Na_2SO_4 electrolytes) aqueous solution in a 5 × 5 cm size thin layer type cell (Cell 2) comprising a nanoporous TiO_2 thin film coated FTO photoanode and a Pt-black electrodeposited FTO cathode with a 0.5-cm thick spacer put between the two electrodes; the cell volume for the liquid was 4 × 4 × 0.5 cm (=8 mL). For this purpose, two different TiO_2 films (A and B) were prepared and investigated as follows: (A) Commercially available Ti-nanoxide T/SP paste (average particle size 13 nm, purchased from Solaronics Co., Ltd.) was coated on an FTO conducting glass by a squeeze coating method. For this, an adhesive tape (thickness about 70 μm) was used as a spacer to adjust the TiO_2 film thickness to around 10 μm after calcination. The deposited TiO_2 film was dried at room temperature, and then calcined at 450 °C for 30 min. (B) TiO_2 (F5, average particle size 20 nm, from Showa Denko Co., Ltd.) was used instead of P-25, the same as the method as that described in the Materials section, but without mixing in a

mortar and without sonication, so as to prepare a rough TiO_2 porous film that does not exhibit good photoanode performance for the BPCC.

As for the instruments, an HZ-3000 automatic polarization system (Hokuto Denko Co., Ltd.) and a 5020 frequency analyzer (NF Electronic Instruments) were used in the frequency range from 20 kHz to 100 mHz by applying a 10 mV amplitude sine wave under open circuit conditions.

3 Results and discussion

As established in a kind of Schottky junction semiconductor photoelectrochemical system [1–3], excitation of electrons from the valence band (VB) to the conduction band (CB) takes place by irradiation of a semiconductor with a light whose energy is larger than the bandgap of the semiconductor, forming separated holes (in the VB) and electrons (in the CB), and the separated charges can induce oxidation and reduction reactions at the anode and the cathode, respectively (for titanium dioxide; $TiO_2 + h\nu \rightarrow h^+$ (VB in TiO_2) + e^- (CB in TiO_2)).

First, an ammonia (NH_3) aqueous solution was photodecomposed at room temperature (25 °C) by using a nanoporous TiO_2 film photoanode in combination with an O_2-reducing Pt cathode resulting in simultaneous generation of electrical power. The cyclic voltammogram (CV) of a nanoporous TiO_2 film photoanode in a 10 M NH_3 aqueous solution (pH 12) under 1 atm O_2 atmosphere at 25 °C under both dark and irradiation is shown in Fig. 1a.

The CV under irradiation exhibited clear photoanodic currents. Although the photocurrent increased gradually with time, it reached a constant value. Such first-stage increase of the photocurrent was often observed also for other compounds, which could be interpreted by direct electron injection into the CB of the TiO_2 from the active radical species formed by oxidation of the substrate compound by the photogenerated holes in the TiO_2. The CV curves showed some hysteresis, which could be ascribed to some slow step(s) among the photoelectrochemical processes probably due to the multi-electron nature of the ammonia decomposition to N_2 (Eq. 1) and/or O_2 (Eq. 2) reduction.

$$\text{Anode} : 2NH_3 + 6h^+ \rightarrow N_2 + 6H^+ \tag{1}$$

$$\text{Cathode} : 3/2O_2 + 6H^+ + 6e^- \rightarrow 3H_2O \tag{2}$$
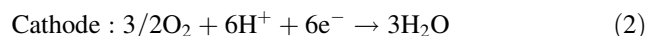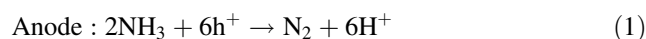
The photocurrent–photovoltage (J–V) characteristics for the ammonia photodecomposition measured by a two electrodes system are shown in Fig. 1b, giving open circuit photovoltage (V_{oc}) 0.87 V, short circuit photocurrent density (J_{sc}) 0.39 A cm^{-2}, and fill factor (FF) 0.65, where FF is the ratio of the real maximum electrical power output per theoretical maximum power output (=$V_{oc} \times J_{sc}$) estimated from the J–V curve (Fig. 1b) under irradiation. In the previous report, we found that NH_3 is decomposed into N_2 and H_2 at the almost theoretical 1/3 molar ratio under Ar atmosphere, while producing photocurrent by using the same cell system [9]. It should be noted here that the J-V characteristics of the N_2/H_2-producing system reported earlier by our group operated under Ar atmosphere were
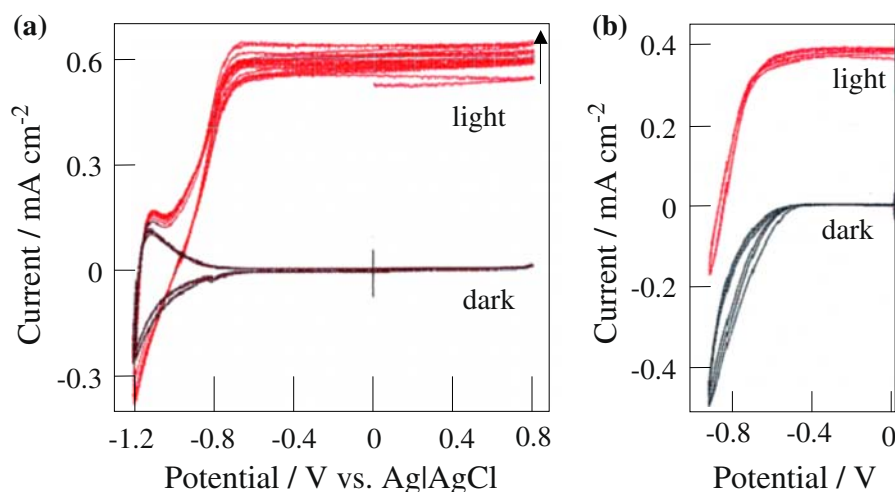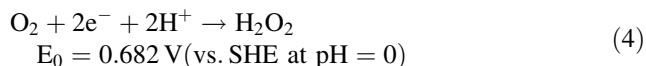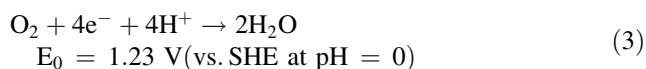

Fig. 1 a Cyclic voltammograms (CVs) of a 10 M NH_3 (+0.1 M Na_2SO_4) aqueous solution (pH 14.5) at a nanoporous TiO_2 film photoanode in combination with an O_2-reducing Pt-black/Pt cathode under 1 atm O_2 atmosphere at 25 °C both under dark and irradiation at the light intensity of 505 mW cm^{-2} (UV light 40 mW cm^{-2}). Scan rate 20 mV s^{-1}; sweep direction, 0 V → 0.8 V → −1.2 V → 0 V. The *inset arrow* shows the direction of the change with time. **b** Corresponding J–V characteristics of a two-electrode system under dark and irradiation. Scan rate 20 mVs^{-1}; sweep direction, 0 V → 0.2 V → −0.9 V → 0 V. J_{sc} = 0.39 mA cm^{-2}, V_{oc} = 0.87 V, and FF = 0.65

only poor in comparison with the present BPCC conducted under O_2 atmosphere. This is because the theoretical maximum cell voltage is only 0.06 V for the N_2/H_2-producing system calculated based on the conduction band edge (E_{CB}) of the TiO_2 (−0.77 V vs. SHE at pH 12, as estimated from the value of E_0 = −0.06 V vs. SHE at pH 0 [10]) and the redox potential for the H^+/H_2 (−0.71 V vs. SHE at pH 12). In contrast, the theoretical maximum cell voltage of the present BPCC operated under O_2 is 1.29 V and N_2 was evolved during the photoelectrochemical process with simultaneous consumption of O_2, but H_2 was not formed under this condition. One reason for the V_{oc} (0.87 V) of only 2/3 of the theoretical V_{oc} (1.29 V) in Fig. 1b could be the mixing of different reaction mechanisms in the first step of O_2 reduction at the cathode as shown by the Eqs. 3 and 4.

$$O_2 + 4e^- + 4H^+ \rightarrow 2H_2O$$
$$E_0 = 1.23 \text{ V} (\text{vs. SHE at pH} = 0) \quad (3)$$

$$O_2 + 2e^- + 2H^+ \rightarrow H_2O_2$$
$$E_0 = 0.682 \text{ V} (\text{vs. SHE at pH} = 0) \quad (4)$$

With the 4 e^- process in Eq. 3 the theoretical cell voltage is 1.29 V, and with the 2 e^- process in Eq. 4 it is only 0.74 V. It is inferred from the obtained V_{oc} of 0.87 V that the main O_2 reduction mechanism taking place at the cathode is the 2 e^- process represented by Eq. 4.

Since, the N_2 formation is a 6 e^- process, and O_2 reduction to H_2O should finally be a 4 e^- process, since H_2O_2 can easily be reduced to H_2O at the cathode reaction, the theoretical molar ratio of (N_2 evolved/O_2 consumed) should be 2/3. In the first-stage of the BPCC reaction, this ratio was slightly larger than this value probably, since the 2 e^- reduction of the formed H_2O_2 to H_2O is delayed, but in the later stage this ratio approached the 2/3 theoretical ratio, since the formed H_2O_2 works as an acceptor to finally be reduced to H_2O. The BPCC reaction mechanism of ammonia can be represented by Fig. 2. The UV light excitation of TiO_2 produces electrons and holes in the CB and VB, respectively, then the holes oxidize NH_3 to N_2, and the electrons are transported to the cathode through the outer circuit to reduce O_2 at the Pt cathode mainly by the reduction of O_2 to H_2O_2 at first and then by further reduction of H_2O_2 to H_2O. In this system, V_{oc} is determined by the potential difference between E_{CB} of TiO_2 photoanode and the redox potential of O_2 reduction at the cathode.

Many biomass-related compounds were photodecomposed by the present nanoporous TiO_2 photoanode in combination with an O_2-reducing cathode with simultaneous generation of electrical power, if they are either liquid or soluble/suspended in water, i.e., they can be used as a direct fuel for the present BPCC. The CVs of the TiO_2 photoanode in a liquid HCOOH containing 0.1 M Na_2SO_4
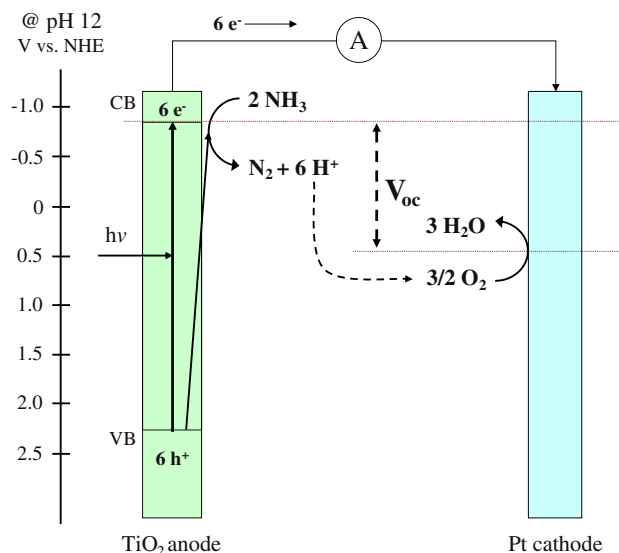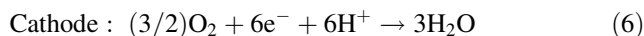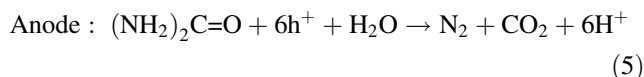

Fig. 2 Potential diagram for the photodecomposition of ammonia at pH 12 with theoretical open circuit photovoltage of V_{oc}

under O_2 atmosphere both under dark and irradiation are shown in Fig. 3a. The CV under irradiation exhibited clear photoanodic currents. Although the increase of the photocurrent in the initial stage of the CV was slower than that of the ammonia (Fig. 1a), the final photocurrent value (4 mA cm^{-2}) was seven times as high as the ammonia. The J–V characteristics of the formic acid (by a two-electrode system) are shown in Fig. 3b, giving $V_{oc} = 0.62$ V, $J_{sc} = 1.40$ A cm^{-2}, and $FF = 0.30$. Figure 3 shows that the formic acid can be used as a direct fuel of the BPCC similarly to ammonia. Although the BPCC characteristics of HCOOH were worse than ammonia in V_{oc} and FF, the J_{sc} value was about three times as high as that of the ammonia.

The J–V characteristics of urea (($NH_2)_2C=O$) in the BPCC are shown in Fig. 4, giving $V_{oc} = 0.6$ V, $J_{sc} = 0.38$ mA cm^{-2}, and $FF = 0.26$. The urea decomposition would take place via NH_3 formation as show by the Eqs. 5, 6, and 7:

$$\text{Anode}: (NH_2)_2C=O + 6h^+ + H_2O \rightarrow N_2 + CO_2 + 6H^+ \quad (5)$$

$$\text{Cathode}: (3/2)O_2 + 6e^- + 6H^+ \rightarrow 3H_2O \quad (6)$$

The J–V characteristics showed some hysteresis, which could be ascribed to some slow steps among the photoelectrochemical processes due to a multi-electron reaction (6 e^- per molecule), the same as mentioned above in the ammonia case.

The CVs of a nanoporous TiO_2 film photoanode in a pure methanol containing 0.1 M tetrabutyl ammonium perchlorate (TBAP) electrolytes under O_2 atmosphere both
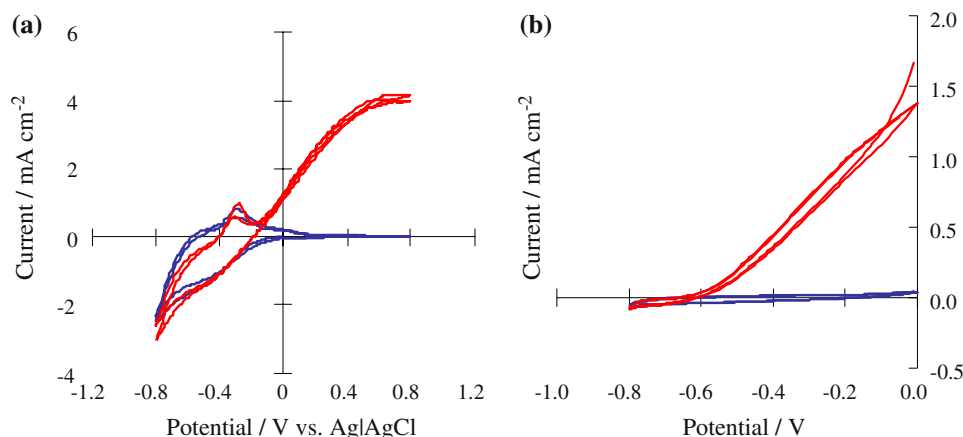
Fig. 3 **a** Cyclic voltammograms (CVs) of a liquid formic acid (+0.1 M Na$_2$SO$_4$) at a nanoporous TiO$_2$ film photoanode in combination with an O$_2$-reducing Pt-black/Pt cathode under 1 atm O$_2$ atmosphere at 25 °C both under dark and irradiation at the light intensity of 505 mW cm^{-2}. Scan rate 20 mV s^{-1}; sweep direction, 0 V → 0.8 V → −0.8 V → 0 V. **b** Corresponding J–V characteristics of a two-electrode system under dark and irradiation. Scan rate 20 mV s^{-1}; $J_{sc} = 1.38$ mA cm^{-2}, $V_{oc} = 0.64$ V, and $FF = 0.22$
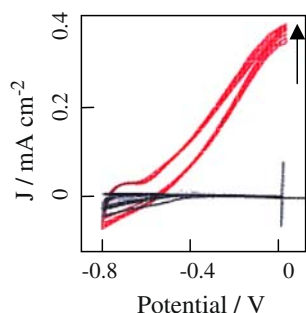

Fig. 4 BPCC characteristics under dark and irradiation at TiO$_2$ (P-25) nanoporous electrode soaked in an aqueous solution of 5.0 M urea (+0.1 M Na$_2$SO$_4$) with a Pt/Pt-black counter electrode, measured at the scan rate of 20 mV s^{-1} under O$_2$ atmosphere. Light intensity, 450 mW cm^{-2}

under dark and irradiation are shown in Fig. 5a. The CVs of a nanoporous TiO$_2$ film photoanode in methanol under air both under dark and irradiation are shown in Fig. 5b. The CVs under irradiation in Fig. 5a, b exhibited clear photoanodic currents, both being saturated around 3 mA cm^{-2}, which demonstrates that the O$_2$ concentration in air is sufficient for the O$_2$ reduction at the Pt cathode for the liquid methanol most probably due to the high solubility of O$_2$ in methanol that is about one order higher than that in water. It is important in our BPCC that organic compounds can be entirely decomposed into CO$_2$ (and N$_2$) as reported earlier [6–9]. The methanol decomposition (6 e$^-$ process) is represented by the Eqs. 7 and 8.

Anode : $CH_3OH + H_2O + 6h^+ \rightarrow CO_2 + 6H^+$ (7)

Cathode : $3/2O_2 + 6e^- + 6H^+ \rightarrow 3H_2O$ (8)
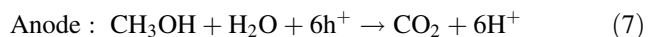
The decomposition product from methanol was analyzed by photodecomposing it in a BPCC using an airtight cylindrical cell with 1 mM MeOH aqueous solution (+0.1 M Na$_2$SO$_4$) (5 mL) under white light irradiation at the intensity of 505 mW cm^{-2}. After 40 h irradiation 120 μL CO$_2$ was formed that corresponds to decomposition of 98% MeOH demonstrating almost quantitative methanol decomposition to CO$_2$.

Cyclic voltammogram was measured in a mixture of methanol and water. The CVs of a nanoporous TiO$_2$ film photoanode in methanol:water (1:1) and methanol:water (1:5) solution under air are shown in Fig. 6a,b, respectively. In Fig. 6a, the saturated photoanodic current value (3.8 mA cm^{-2}) is larger than that in pure methanol (3.0 mA cm^{-2} in Fig. 5b) probably due to the presence of water, since water is needed for the reaction as shown in Eq. 7. However, the photoanodic current value (2.8 mA cm^{-2}) in methanol:water (1:5) solution is smaller than that in pure methanol (3.0 mA cm^{-2}) probably due to the low methanol concentration. An optimum methanol concentration condition in water would therefore exist to generate the maximum photocurrent.

The J–V characteristics of a methanol BPCC under O$_2$ are shown in Fig. 7 as an example, and the BPCC characteristics in pure methanol and methanol:water (1:1) mixture are summarized in Table 1. Although the FF was slightly lower for the pure methanol, both the systems showed similar characteristics. The J–V characteristics of methanol under O$_2$ with a solar simulator (AM 1.5G, 100 mW cm^{-2}, UV light intensity was 8 mWcm^{-2}) irradiation are shown in Fig. 8. It should be noted that the BPCC showed clear photocurrents, demonstrating the effectiveness of solar irradiation for generating electrical power.

The CVs of a nanoporous TiO$_2$ film photoanode in pure ethanol containing 0.1 M TBAP under O$_2$ atmosphere both

Fig. 5 Cyclic voltammograms of methanol (+0.1 M TBAP) at a nanoporous TiO_2 film photoanode in combination with an O_2-reducing Pt/Pt-black cathode under **a** 1 atm O_2 and **b** air atmosphere at 25 °C both under dark and irradiation at the light intensity of 505 mW cm^{-2}. Scan rate, 10 mV s^{-1}
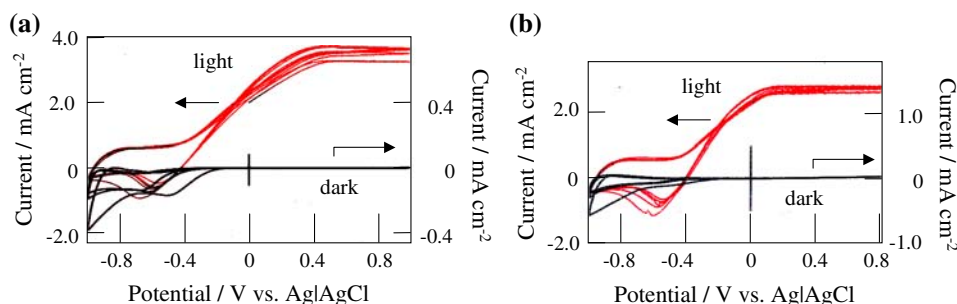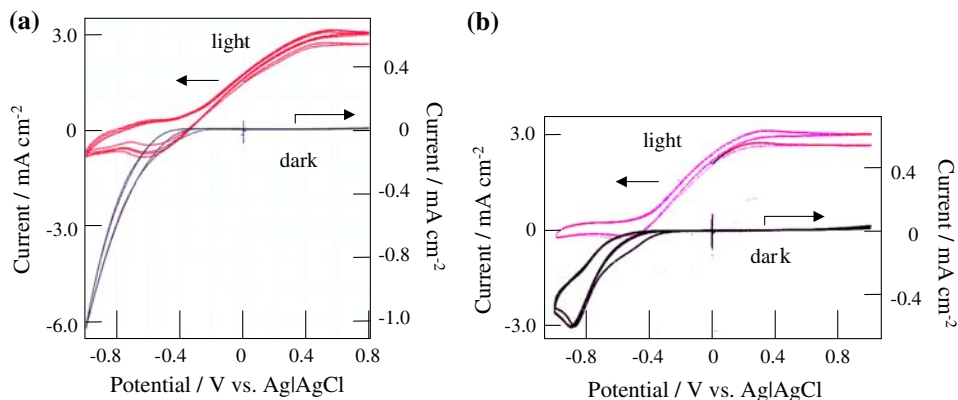

Fig. 6 Cyclic voltammograms of methanol aqueous mixtures (+0.05 M TBAP and 0.05 M KNO_3) at a nanoporous TiO_2 film photoanode in combination with an O_2-reducing Pt/Pt-black cathode under air atmosphere at 25 °C both under dark and irradiation at the light intensity of 505 mW cm^{-2}. Scan rate, 10 mV s^{-1}. **a** 50% methanol aqueous solution. **b** 20% methanol aqueous solution

Fig. 7 BPCC characteristics under dark and irradiation at TiO_2 nanoporous electrode soaked in methanol (+0.1 M TBAP), with a Pt/Pt-black counter electrode, measured at the scan rate of 10 mV s^{-1} under O_2 atmosphere. Light intensity, 505 mW cm^{-2}

Fig. 8 BPCC characteristics under dark and irradiation at TiO_2 nanoporous electrode soaked in methanol (+0.1 M TBAP), with a Pt/Pt-black counter electrode, measured at the scan rate of 10 mV s^{-1} under O_2 atmosphere with a solar simulator (AM 1.5G, 100 mW cm^{-2}) irradiation (UV light 8 mW cm^{-2}). $J_{sc} = 0.31$ mA cm^{-2}, $V_{oc} = 0.44$ V, and $FF = 0.27$
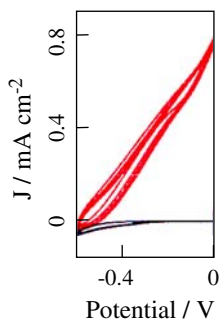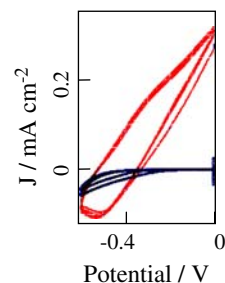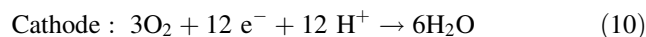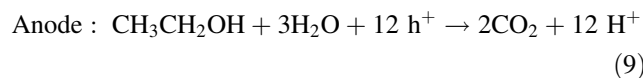
Table 1 PFC characteristics of methanol and methanol/water mixture solution (+0.1 M TBAP) by using nanoporous TiO_2 photoanode (1 × 1 cm^2) and Pt/Pt-black foil cathode (1 × 1 cm^2) in a one compartment cell with a 500 W xenon lamp (505 mW cm^{-2}) irradiation

Solvent (conc./M)	V_{oc}/V	J_{sc}/mA cm^{-2}	FF
None	0.54	0.80	0.23
Water (13)	0.44	0.76	0.28

Anode : $CH_3CH_2OH + 3H_2O + 12\ h^+ \rightarrow 2CO_2 + 12\ H^+$ (9)

Cathode : $3O_2 + 12\ e^- + 12\ H^+ \rightarrow 6H_2O$ (10)

The CVs of Fig. 9a, b exhibited clear photoanodic currents, but the increase of the photocurrent was slow probably due to the unfavorable 12 e^- multi-electron oxidation process of the ethanol decomposition to CO_2. Although the oxygen partial pressure of Fig. 9b is one-fifth of that in the Fig. 9a,

under dark and irradiation are shown in Fig. 9a, and those under air are shown in Fig. 9b. The ethanol decomposition to CO_2 (12 e^- process) is a 12-electron process, and can be represented by Eqs. 9 and 10.

Fig. 9 Cyclic voltammograms of ethanol (+0.1 M TBAP) at a nanoporous TiO_2 film photoanode in combination with an O_2-reducing Pt/Pt-black cathode under **a** 1 atm O_2 and **b** air atmosphere at 25 °C both under dark and irradiation at the light intensity of 505 mW cm^{-2}. Scan rate; 10 mV s^{-1}
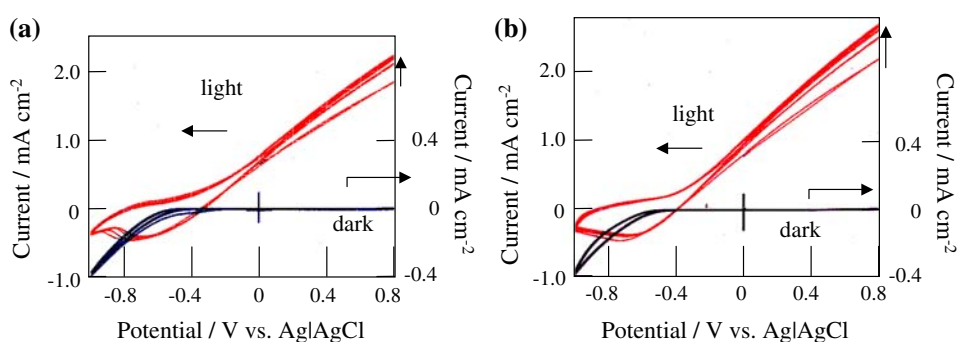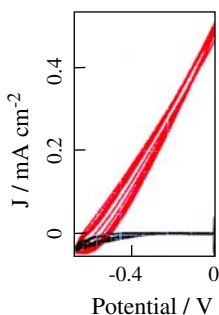

Fig. 10 BPCC characteristics under dark and irradiation at TiO_2 nanoporous electrode soaked in ethanol (+0.1 M TBAP) with a Pt/Pt-black counter electrode, measured at the scan rate of 10 mV s^{-1} under O_2 atmosphere. Light intensity, 505 mW cm^{-2}

the photoanodic current of Fig. 9b is similar to that of Fig. 9a, suggesting that the process is mainly determined by the multi-electron photo-oxidation of ethanol at the photoanode. The J–V characteristics of ethanol under O_2 are shown in Fig. 10.

The BPCC characteristics of ethanol and methanol under O_2 are compared in Table 2. The higher electrical power generation ($V_{oc} \times J_{sc} \times FF$) by methanol could be ascribed to its easier 6 e$^-$ process for the methanol decomposition than the 12 e$^-$ process of ethanol.

The charge transport process in the BPCC was investigated by alternating current impedance spectroscopy by using a thin layer type cell that has an open air structure. Glycine was adopted as the material due to its stability in the open air cell. As mentioned in the Experimental section, two different BPCCs were fabricated for this purpose: one is a conventional good performance cell using a well mixed commercially available TiO_2 paste (A; with average 13 nm size TiO_2 particles, see Experimental), and another is a worse performance cell (B) fabricated without mixing well the materials of TiO_2 (average 21 nm size), acetylacetone, water, and Triton X-100. The I–V characteristics of these

Table 2 PFC characteristics of methanol and ethanol solution (+0.1 M TBAP) by using nanoporous TiO_2 photoanode (1×1 cm^2) and Pt/Pt-black foil cathode (1×1 cm^2) in a one compartment cell with a 500 W xenon lamp (505 mW cm^{-2}) irradiation

Fuel	V_{oc}/V	J_{sc}/mA cm^{-2}	FF
EtOH	0.49	0.52	0.25
MeOH	0.54	0.80	0.23

two cells with a 0.5 M glycine substrate (+0.1 M Na_2SO_4 electrolytes) aqueous solution are shown in Fig. 11. Cell A showed much better conversion characteristics than Cell B. As for the photodecomposition product from glycine, 1 mM glycine was photodecomposed by the same method as that of methanol described above, confirming formation of both CO_2 and N_2 at almost the theoretical $CO_2/N_2 = 4/1$ molar ratio resulting in 48% decomposition yield after 42 h irradiation.

The alternating current impedance spectra from 20 kHz to 100 mHz for both Cells A and B under irradiation at the 100 mWcm^{-2} light intensity are shown in Fig. 12a, b. Figure 12b shows magnified curves in the high frequency region from 20 kHz to ca. 10 Hz of Fig. 12a. The two curves exhibited a similar trend, but clearly differ. The curves were interpreted as follows:

(1) The plots could not be fitted well by "one-component and two-component semicircles" analysis, but they were fitted well by "three-component semicircles" analysis. The equivalent circuit for the cells shown in
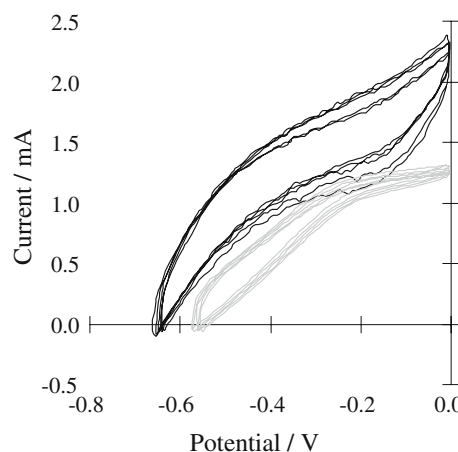

Fig. 11 BPCC characteristics of A (*black line*) and B (*gray line*) TiO_2 photoanodes (16 cm^2) soaked in a 0.5 M glycine aqueous solution (+0.1 M Na_2SO_4), with an FTO/Pt-black as a cathode, measured at the scan rate of 10 mV s^{-1} under air. Light intensity, 100 mW cm^{-2} from a Xe lamp (with HA-50 IR cutoff filter)

Fig. 12 AC impedance spectra for 0.5 M glycine in water in a thin layer type-BPCC with (*shaded square*) A and (*shaded diamond*) B photoanodes at the open circuit potential under air. Light intensity, 100 mW cm^{-2} from a Xe lamp (with HA-50 IR cutoff filter). **a** Frequency range from 20 k Hz to 100 m Hz. **b** Magnified view of (**a**) at the high and middle frequency ranges
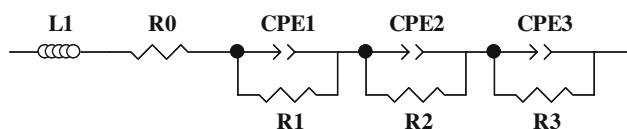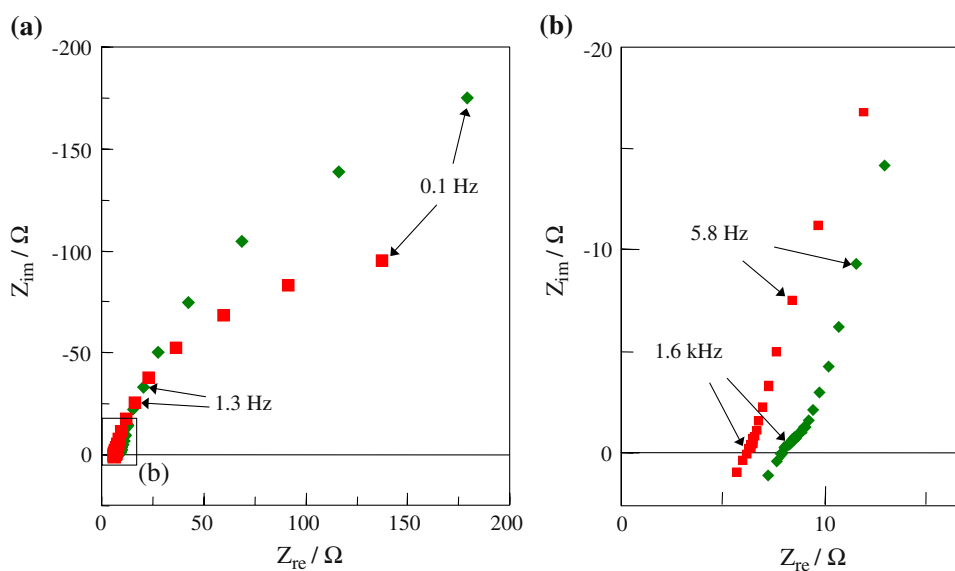

Fig. 13 Equivalent circuit to analyze the alternating current impedance spectra of Fig. 12. About the parameters see the text

Fig. 13 gave the best fitting of the impedance spectra, where the parameters indicate the following items:

*L*1: Mutual inductance of the wires connecting potentiostat and the cell

*R*1: Resistances at FTO conducting layer/TiO$_2$ and FTO conducting layer/Pt interfaces and in bulk solution

*R*2: Resistances at TiO$_2$ and Pt grain boundaries

*R*3: Resistances for charge transfer at TiO$_2$/solution and Pt/solution interfaces and for molecular diffusion in the double layer on both the electrode surfaces

*CPE*1: Constant phase elements related to double layer capacitances at FTO/TiO$_2$ and FTO/Pt interfaces

*CPE*2: Constant phase elements related to double layer capacitances at TiO$_2$ and Pt grain boundaries

*CPE*3: Constant phase elements related to double layer capacitances at TiO$_2$/solution and Pt/solution interfaces and affected by the diffusion of reactive species in the double layer

(2) The computational analysis results of double layer capacitances (*C*1, *C*2, and *C*3) and of charge transfer resistances (*R*1, *R*2, and *R*3) conducted by the instrument based on the "three-component semicircles" are shown in Table 3.

(3) Among the resistances of *R*1, *R*2, and *R*3, *R*3 is the major charge transfer resistance due to the reactions at the photoanode and the cathode, while *R*2, the resistance at the TiO$_2$ and Pt grain boundaries, is the smallest, showing that the cell performance is determined mainly by the chemical reactions at the TiO$_2$ and Pt electrodes by holes and electrons, respectively, but the resistances at the grain boundaries and at the FTO/TiO$_2$ and FTO/Pt interfaces and in bulk solution are almost negligible.

(4) When comparing the resistances of *R*1, *R*2, and *R*3 between A and B, A gave smaller values than B for all the resistances, which is the natural consequence of the TiO$_2$ film made of well-mixed and smaller sized TiO$_2$ paste (for A) and the poorly mixed and larger sized TiO$_2$ paste (for B).

Table 3 Fitted parameters based on the equivalent circuit (Fig. 13) in the electrochemical impedance spectroscopy for a 0.5 M glycine aqueous solution thin layer type-BPCC (1 cm × 1 cm) with A and B photoanodes, measured at the open circuit potentials

TiO$_2$ film	$C1\times10^{-7}$ (F)	f_{max} (Hz)	$R1$ (Ω)	$C2\times10^{-4}$ (F)	f_{max2} (Hz)	$R2$ (Ω)	$C3\times10^{-3}$ (F)	f_{max3} (Hz)	$R3$ (Ω)
A	3.89	63552	6.44	3.55	2298	0.20	6.29	0.11	223
B	1.92	99734	8.30	9.51	100	1.67	5.05	0.08	415

f_{max} shows top position frequency of the corresponding semicircle

Thus, the different conversion efficiencies in Fig. 13 were interpreted well by the alternating current impedance spectroscopy.

4 Conclusion

Photoelectrochemical decomposition of bio-related compounds with a nanoporous TiO_2 film photoanode and an O_2-reducing cathode was investigated to simultaneously generate electrical power. The bio-related compounds were photodecomposed by the present BPCC, when they are either liquid or soluble in water, i.e., they can be used as a direct fuel for the BPCC. Aqueous solutions of bio-related compounds such as ammonia, formic acid, urea, methanol, ethanol, and glycine were investigated for the BCPP under O_2 of air. It was demonstrated that varieties of bio-related compounds can be photodecomposed and simultaneously generate electrical power by the BPCC. The alternating current impedance spectroscopy showed that the charge transfer processes from the photoanode and the cathode into the solutes (organic compounds and O_2, respectively) compose the major resistances for the cell performance.

References

1. Gerischer H (1960) Z Phys Chem 26:325
2. Honda K, Fujishima A (1972) Nature 238:37
3. Matthews RW (1991) In: Pelizzetti E, Scheavello M (eds) Photochemical conversion and storage of solar energy. Kluwer Academic Publishers, Dordrecht, pp 427–449
4. Kaneko M, Okura I (eds) (2002) Photocatalysis—science and technology. Kodansha/Springer, Tokyo
5. O' Regan B, Graetzel M (1991) Nature 353:737
6. Kaneko M, Nemoto J, Ueno H, Gokan N, Ohnuki K, Horikawa M, Saito R, Shibata T (2006) Electrochem Commun 8:336
7. Nemoto J, Horikawa M, Ohnuki K, Shibata T, Ueno H, Hoshino M, Kaneko M (2007) J Appl Electrochem 37:1039
8. Kaneko M, Ueno H, Ohnuki K, Horikawa M, Daito RS, Nemoto J (2007) Biosens Bioelectron 23:140
9. Kaneko M, Gokan N, Katakura N, Takei Y, Hoshino M (2005) Chem Commun 2005:1625
10. Hagfeldt A, Graetzel M (1995) Chem Rev 95:49